

Analysis of demand and supply of electrical energy in Cameroon: Influence of meteorological parameters on the monthly power peak of south and North interconnected electricity networks

Flora Isabelle Métégam Fotsing^{1,2}, Donatien Njomo¹, René Tchinda²

¹Environmental Energy Technologies Laboratory (EETL), University of Yaounde I, PO Box 812, Yaounde, Cameroon

²Laboratory of Industrial Systems and Environment of the University of Dschang, PO BOX 96, Dschang, Cameroon

Email address:

fotsing85@yahoo.fr (I. Fotsing), dnjomo@usa.net (D. Njomo), ttchinda@yahoo.fr (R. Tchinda)

To cite this article:

Flora Isabelle Métégam Fotsing, Donatien Njomo, René Tchinda. Analysis of Demand and Supply of Electrical Energy in Cameroon: Influence of Meteorological Parameters on the Monthly Power Peak of South and North Interconnected Electricity Networks. *International Journal of Energy and Power Engineering*. Vol. 3, No. 4, 2014, pp. 168-185. doi: 10.11648/j.ijepe.20140304.12

Abstract: Following the unbalanced provision between supply and demand of electrical energy in Cameroon, it is necessary to perform an analysis of the data since it can provide essential information for an optimal management of the power supply system. This study presents on the one hand an analysis of electrical energy demand and supply in Cameroon, and, on the other hand, the modeling of the monthly peak of the main interconnected network in Cameroon, namely South Interconnected Networks (RIS) and North (RIN) networks using econometrical methods. Meteorological parameters (monthly maximal temperatures and humidity) are considered as exogenous variables of this application. Following the seasonality observed during various months, the introduction of terms of monthly seasonal as well as an average coefficient C_i peculiar to each month will also be introduced into the linear regression model to evaluate the most suitable one for this modeling. From the above analysis, it appears that meteorological parameters have a significant influence on the monthly peak in both networks. As well as the coefficients of these parameters are not the most significant of the various models, the absence of these parameters in different models leads to an increase Akaike (AIC) and Schwartz (SC) criteria. However, the best model is based on the minimum AIC and SC. The monthly peak in both systems is observed at the same time (20h) and one a working day. This peak may be influenced by other parameters such as the return to households and their consumption pattern, the type of equipment they use amongst other.

Keywords: Monthly Peak, Linear Regression Models, Meteorological Parameters, Network RIS and RIN, Modeling, Demand and Supply

1. Introduction

Load demand of electricity served by a system of power is not constant in a day; it has maximum values at a given time, which is known as a peak. Electricity was produced and managed in Cameroon till 2013 by an American Company called AES SONEL and since 2014 by an English company called ACTIS. It is produced from three hydroelectric power stations and nine thermal power plants connected to the network. Most of these Thermal power plants are mainly used for the management of the peak (6 to 10 PM) with the peak observed most of the time at 8PM and sometime at 7PM. Strong demand during the peak

causes decreases the voltage and significant outages that can cause extensive damage to both the population and the economy. In order to reduce the gap between electricity supply and demand, it is necessary to analyze factors that can influence the quantity and quality of demand in order to identify the parameters impacting it heavily.

However, the monthly peak can be influenced by meteorological parameters. Therefore, more information about this monthly peak could help the company that produces the electricity to better manage its means of production. This could also help to advise the government on energy policy to be put in place to meet the population demand of electricity.

The works presented in this article are intended to analyze and to model the supply and the demand of electricity energy from Cameroon electricity networks. This modeling is based on two types of data, namely the monthly peak consumption and the seasonal variations in meteorological parameters data. However, the specificity of this study results in the quality and variety of sources of supply that meet with many uncertainties, the demand for power consumption. These variations in production affect how Cameroon meets the cyclical demand for its electricity. Different patterns of consumption of electrical energy are thus presented for the two main networks that make the Cameroon electrical park. These models depend in particular on the frequency, the seasonality and the peculiar dynamics of consumption of electricity in the country.

Several studies have been made on the request of the peak load. Reference [17] has implemented strategies to reduce peak demand in southwest deserted region of the United States of America thanks to the cooling load. Reference [7] analyzes the impact of natural light on the peak in Hong Kong. Reference [15] performed an analysis in a residential area in Brazil to satisfy the electricity demand while reducing the peak load. Reference [3] shows that the temperature and seasonality influence the consumption of electricity in Spain. Reference [10] evaluates the influence of economic variables on electricity consumption in Northern Cyprus. Reference [18] analyzes the use of renewable energy in India in order to reduce the load of existing peak. Reference [5] modeled the electricity consumption in Togo using the meteorological parameters as exogenous variables. Reference [21] evaluates the characteristics of the demand of seasonal electricity peak observed in a commercial area in Japan using meteorological parameters as exogenous variables thanks to econometric models.

In this study, we first analyze the demand and supply of electric energy in Cameroon, and then we investigate the monthly peak consumption of the Cameroon major electric networks. The investigations are carried out in the evening because the peak is observed at 8PM in both networks. Seasonal demand patterns are used as a basis for composing the linear regression model. From there, the direct link between the peak load and all the variables in each season can be verified. The typical relationship between seasonal demand peak and the meteorological variables is represented and further analysis carried out on them. The results obtained in this study can give more insight to identify the characteristics between the peak demands and variables that led to it. This research work can contribute to a better operation of power systems. It could become a fundamental work for the seasonal planning decisions necessary to improve the gap between demand and supply during the peak in Cameroon.

This paper is organized as follows; Section 1 presents the analysis of demand in the RIS and RIN; the analysis of supply is presented in Section 2. Data of modeling are described in Section 3. Thereafter, Section 4 presents the

various models proposed for the RIS and INR. Section 4 presents the results of regression models. The conclusion and comments are presented in Section 5.

2. Demand and Supply Analysis in the RIS and RIN

2.1. Demand Analysis in the RIS and RIN

2.1.1. Demographic Indicators of RIS and RIN

In the 21st century, the population of Cameroon is estimated at about 21.7 million inhabitants. Its density is 44.8 inhabitants per km² with a natural increase of 2.5% in 2012 according to World Bank. Cameroon is the most populous country in Central Africa because it has 48% of the total population of the five countries in this region, followed by Chad (23%); CAR (11%); Congo (); Gabon (5%) and Equatorial Guinea (4%). Cameroon has a very young population with 42.5% of young people under age 15 and 19.4% of residents who are between 24 years and older.

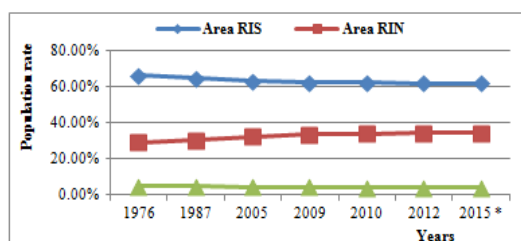
There are three electricity networks to cover the Cameroon space.

- The South interconnected network (RIS): The six areas covered are: Centre, Littoral, West, Northwest, Southwest and South regions.
- The North interconnected network (RIN): it covers three areas: Adamawa, North and Far North regions.
- The Eastern network: this network is not connected; it covers only the East region of Cameroon.

The evolution of the population of the Eastern zone is decreasing due to the under populating caused by a high coverage of the swampy forest. The population of the area of RIN has undergone a light increase from 21.9% to 34.4%, while the population of the area of RIS has weakly decreased from 66.1% to 61.9% between 1976 and 2012. The demographic weight is more pronounced in the Centre region in 2012 with 18.4%, followed by the Far North (18%) and the Littoral regions (15%). The causes of this demographic development in the area of RIS can be explained from such factors as the existence of the political and economic capital respectively at the Centre and Littoral regions meanwhile in the area of the RIN it can be justified by a high concentration of the population in the far North region .

In terms of space and knowing the subdivision of Cameroon into ten administrative regions, we note that the demographic weight is the highest in the Central region (about 18.4% in 2012), which hosts the political capital Yaoundé, representing an important economic urban center. The other regions also populated are the Far North and the Littoral region with respectively about 18% and 15% of the total population of the country in 2012. The Littoral region hosts the main economic center of Cameroon, the city of Douala, with its important commercial sea port which is also a maritime hub in the Central African region. The democratic weights of the Centre and Littoral regions are justified by the relatively high concentration of urban areas

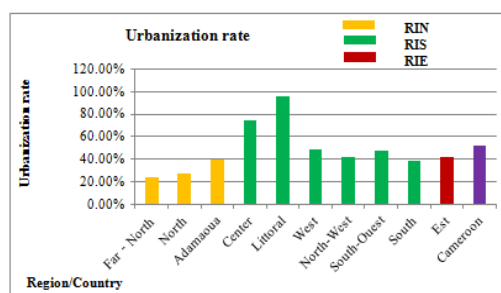
in these two regions and collective economic and social centers offering employment opportunities. The proportion of the rural population in Cameroon continues to remain significant (48% in 2010) [2] despite a clear downward trend since 1976. Urbanization rate of the population in Cameroon has however increased from 28.5% in 1976 to 52% in 2010, reflecting a sustained growth of the total urban population, with an average annual growth rate (CAGR) estimated at 4.6% for the whole period from 1976 - 2010 against 1.5% average annual growth of the rural population during the same period. *Figure 1.* shows evolution of the registered demographic distribution in Cameroon by large area.



Source: Statistical Yearbook 2010 Cameroon - INS

Figure 1. Evolution of the Registered Demographic distribution in Cameroon by large area

The urbanization rate in various areas is presented as follow: 27.6% for the NIR, 66% for RIS and 41.6% for the RIE [Statistical Yearbook 2010 Cameroon - INS]. In 2010, the global urban population is distributed between the three areas of the country as follow: RIS area 78.7%, RIN area 18% and RIE area 3.3%. *Figure 2* shows evolution of the urbanization rate by region.

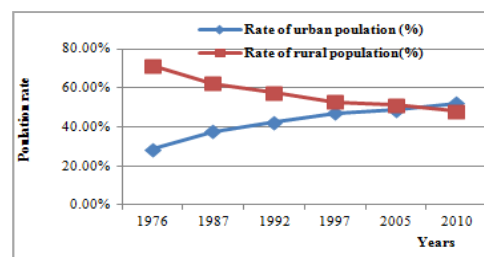


Source: Statistical Yearbook 2010 Cameroon - INS

Figure 2. Evolution of the urbanization rate by region

In terms of poverty, the overall proportion of the Cameroonian population living below the poverty line was estimated in 2007 to about 40%; the index of severity of poverty among the population nationwide has also recorded a decline from 5.6% in 2001 to 5% in 2007. Poverty rate (% of population living below the poverty line) showed a trend of decrease much more sustained in urban areas than in rural areas, resulting in more job opportunities and more stable incomes in urban areas. According to the available household surveys previously conducted by the INS estimates, the national poverty rate in urban areas has

decreased from 44.4% in 1996 to 12.2% in 2007 and has reduced in rural areas almost from 60% in 1996 to 55% in 2007. *Figure 3* shows evolution of registered urbanization rate of the Cameroonian population.



Source: Statistical Yearbook 2010 Cameroon - INS

Figure 3. Evolution of Registered Urbanization rate of the Cameroonian population.

Poverty is more acute in rural areas and especially in the three regions of the RIN region because the income of the population comes mainly from agriculture. This sector is vulnerable to climate hazards, intermittent income it provides and its agricultural techniques have remained traditional and very little mechanized in several regions of the country. Thus, poverty is most prevalent and pronounced in the labor force groups employed in the informal agricultural sector. Those having formal private or administrative activities appear to be less affected by poverty. These activities are more developed in urban areas and in larger socio economic centers of the country, such as Douala and Yaoundé. Taking into account the demographic changes, the average income per capita nationwide is estimated at current prices of 595 455.1 FCFA / capita in 2010 and recorded over the last decade (2000-2010) a TCAM of 0, 87%.

2.1.2. Cameroon Macroeconomic Indicators

Analysis of the structure of real GDP for the year 2009 shows that the tertiary sector (trade, hotels and restaurants, transport and communication, finance & real estate, administrative services, miscellaneous services) was the main component of the national GDP, estimated at around 47% share. Activities, Especially business, with catering and hotel industries are the backbone of this sector, with a share of 20.1% of total national GDP. This can be explained by the low need of investment compared to other economic sectors.

The secondary sector (mining and extraction (including oil activities), manufacturing, construction, electricity, gas & water) is the second largest economic sector, with an estimated share of nearly 30% of real GDP in 2009. The manufacturing industries represent the sub prime sector with a contribution to the national GDP of about 16%, estimated in the same year.

The primary sector (agriculture, forestry and forest extraction, fishing, hunting and livestock) has meanwhile accounted for less than one quarter of national GDP at a constant price, nearly 23% in 2009. Primary key sub-sector

is subsistence agriculture which would have been 63% of GDP the same year around against respectively 13% for forestry, 12% for livestock & hunting, 6.5% for industrial agriculture and exports and 5.5% for fishing. [23]. *Figure 4.* shows evolution of sectorial GDP and average annual growth rate.

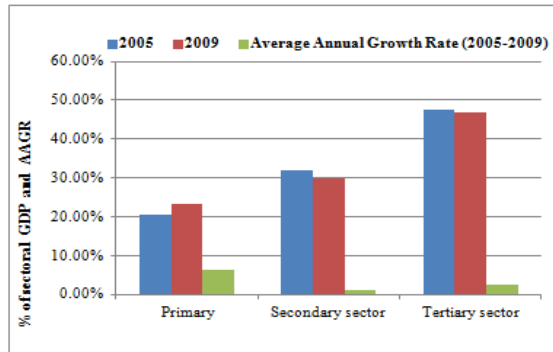


Figure 4. Evolution of sectorial GDP and AAGR

2.2. Analysis of Supply

2.2.1. Electric Power Generation

The electricity generation fleet managed by AES SONEC has three hydroelectric plants, two of them feed the South network (RIS) and 9 thermal plants connected to the grid, including eight (8) debiting on the RIS. At the end of 2011, one could count 26 isolated plants, which 12 built in the regions supplied by the RIS, 8 in the northern areas served by the north network (RIN) and the 6 remaining others were established in the area of East network (eastern region); by analogy to RIN and RIS, the latter will be designated by RIE, especially as it is expected to have a supply of 90 kV from the Lom Pangar dam as from 2016. Thus, over 56% of the workforce electric park is concentrated in the large area of the South (RIS area), with 83% of the main stations connected to the network and 44% of isolated plants; this therefore should reflect the relative importance of the electricity demands in the Great South network. *Table 1* shows the electric energy production (in% of total production).

Table 1. Electric Energy Production (in% of Total Production)

Year /Electric Production	2005	2006	2007	2008	2009	2010	2011	Average share
Hydro - RIS	89,00%	88,70%	85,20%	89,00%	84,80%	86,50%	86,30%	87,10%
Hydro- RIN	5,20%	5,10%	5,10%	4,90%	5,40%	5,40%	5,40%	5,20%
Hydro- (RIN+RIS)	94,20%	93,80%	90,40%	93,90%	90,20%	91,90%	91,70%	92,30%
Thermal- RIS	4,50%	4,80%	8,30%	4,40%	8,10%	6,30%	6,50%	6,10%
Thermal - RIN	2,9 %°	0,2%°		0,1 %°	0,1 %°			0,8 %°
								(per thousands)
Total Thermal (RIN+RIS)	4,50%	4,80%	8,30%	4,40%	8,10%	6,30%	6,50%	6,10%
Total Hydro + Thermal RIS	93,50%	93,50%	93,50%	93,50%	92, 9%	92,80%	92,80%	93,20%
Total Hydro + Thermal RIN	5,20%	5,10%	5,10%	4,90%	5,50%	5,40%	5,40%	5,20%
Total Hydro + Thermal (RIN+RIS)	98,70%	98,60%	98,60%	98,40%	98,30%	98,20%	98,20%	98,40%
Total isolated Thermal - RIS	0,15%	0,16%	0,17%	0,18%	0,16%	0,19%	0,21%	0,20%
Total isolated Thermal - RIE	0,73%	0,77%	0,74%	0,84%	0,94%	0,96%	1,05%	0,90%
Total isolated Thermal - RIN	0,41%	0,44%	0,38%	0,49%	0,55%	0,53%	0,53%	0,50%
Total isolated Thermal (RIN+RIS+RIE)	1,30%	1,40%	1,40%	1,60%	1,80%	1,80%	1,80%	1,60%
overall	100,00%	100,00%	100,00%	100,00%	100,00%	100,00%	100,00%	100,00%

Source: AES SONEC

Hydro electric production accounted for the bulk of domestic production, with over an average of 92% of national electric production managed by AES SONEC from 2005 to 2011. The predominant share of electricity produced by AES SONEC, with an averaging of 87.1% is located in the regions supplied by the RIS. The share of thermal generation plants connected to the grid represented an average of 6.1% of the production of AES SONEC nationwide during the last period, with a maximum of 8.3% obtained in 2007. Isolated thermal power plants yield, in turn, an average of 1.6% of the national production of AES SONEC, with a maximum of 1.8% in 2011 [1]. Isolated plants that have been dismantled had yield roughly a share of about 0.046% on average of the total domestic production.

2.2.2. Non-Synchronous Peak Output

Over the period 2005- 2011, The sum of the peaks from the three hydro electric represents an average of 82.3% of the total peaks of all power plants connected to the grid, with a maximum of 85.2% in 2011 and a minimum of 80 3% in 2005. The share of thermal power plants connected to the grid represents during the same period an average of 17.7% of the total sum of peaks recorded, with a minimum of 14.8% in 2011 and a maximum of 19 7% in 2010. From the above, we see that the share production of heat from thermal power plants has been steadily declining over the same period in favor of hydroelectric generation which grew 5MW over the same period. As previously checked, these grid-connected power plants produce an average of 6.1% of the total energy produced by AES SONEC, confirming the

supporting role in peak power plants connected to the AES-SONEL grid. Most of the power plants contribute much to the national forefront, with the exception of the LPP (Limbe Power Plant) which, alone, produces 10.1% of 17.7%

representing the total contribution of thermal plants connected to network. *Table 2* shows power peak observed by central (in MW).

Table 2. Power Peak Observed by Central (in MW)

Years/ Peak	2005	2006	2007	2008	2009	2010	2011
Hydro- RIS	563	588	603	632	633	655	646
Hydro - RIN	40,4	40,6	41,7	40,1	45,2	46	48,9
Total Hydro- (RIN+RIS)	603	629	645	672	678	701	695
Thermal - RIS	148	149	148	136	157	128	121
Thermal - RIN	0	4,1	0	1,1	0,9		
Total Thermal (RIN+RIS)	148	149	148	137	157	128	121
Total Hydro+ Thermal – RIS	711	737	751	768	790	783	767
Total Hydro. + Thermal – RIN	40	45	42	41	46	46	49
Total Hydro + Thermal (RIS+RIN)	751	782	793	809	836	829	816
Totale Isolated Thermal- RIS	*	*	3,24	2,58	2,45	2,33	2,74
Total Thermal Isolée - RIE	*	*	8,05	8,63	9,44	10,51	11,50
Total Isolated Thermal - RIN	*	*	4,43	5,00	5,63	5,04	5,39
Total Isolated Thermal (RIN+RIS+RIE)	*	*	16,27	26,79	18,18	17,88	19,63
overall			809	835	854	847	836

Source: AES SONEL * Data not shown

Table 3. Determination of Synchronous peaks from RIS and RIN Networks (January 2006 - May 2012)

Years	2006	2007	2008	2009	2010	2011	2012
N RIS Network							
1 Peak RIS (MW)	490,4	514	555	584,8	616,3	666,84	
2 Annual increment per cent (%)		4,8%	8,0%	5,4%	5,4%	8,2%	
3 Date of peak	26 th Dec. (Tuesday)	27 th Dec. (Thursday)	24 th Dec. (Wednesday)	17 th Dec. (Thursday)	16 th Dec. (Thursday)	9 th Dec. (Friday)	
4 time of peak	08PM	08PM	08PM	08PM	08PM	08PM	
5 Load of RIN synchronous with annual peak of RIS (in MW)	35,4	32,2	34,0	37,4	40,0	42,3	
6 Sum of synchronous loads of RIS + RIN with the peak RIS	525,8	546,2	589,0	622,2	656,3	709,1	
7 Annual increment per cent (%)		3,9%	7,8%	5,6%	5,6%	8,1%	
RIN Network							
8 Peak RIN (MW)	39,8	40,5	39,3	44,4	45	49	51,5
9 Annual increment per cent (%)		1,8%	-3,0%	13,0%	1,4%	8,9%	5,1%
10 Date of peak	23 ^h Feb. (Thursday)	07 ^h Mach (Wednesday)	06 ^h Mach (Thursday)	23 ^h Mach (Monday)	17 ^h Feb. (Wednesday)	25 ^h Mach (Wednesday)	13 ^h Mach (Tuesday)
11 time of peak	08PM	08PM	08PM	08PM	08PM	08PM	08PM
12 Load of RIS synchronous with annual peak of RIN (in MW)	426,7	491,8	502,0	494,1	552,2	578,3	582,9
13 Sum of synchronous loads of RIS + RIN with the peak RIN	466,5	532,3	541,3	538,5	597,2	627,3	634,4
14 Annual increment per cent (%)		14,1%	1,7%	-0,5%	10,9%	5,0%	1,1%
RIN + RIS Networks							
15 Sum (Non synchronous) of individual peaks of the two RIS & RIN networks of the same year (in MW)	530,2	554,5	594,3	629,2	661,3	715,8	
Sum of non synchronous /synchronousSomme peaks							
16 Coefficient of de expansion	0,992	0,985	0,991	0,989	0,992	0,991	

Source: Load curves collected AES-SONEL from 2006 to May 2012

2.2.3. Comparison between Non-Synchronous Sum of Peaks and the Synchronous Peak of Each RIN and RIS Networks

The analysis of load curves from 2006 to 2011 and the first term of 2012 enable us to identify and assess the synchronous peak of production centers connected to each RIN and RIS systems, considered separately. The aggregation of load curves enables to determine the overall synchronous peak of the two RIS RIN networks. This aggregation allows us to estimate the expansion coefficients. Table 2.3 summarizes the results of this analysis. The values shown in this table derive from the analysis of load curves received from AES-SONEL on both RIN and RIS networks.

The annual peak of RIS network always takes place over the period studied, the month of December, a working day to 20 hours. This peak has evolved with an average Annual increment percentage of 6.3%. The synchronous network load of RIN with the annual peak of the RIS (same year, same day and same time) was determined and the synchronous sum in MW of the two networks at the forefront of RIS was calculated on lines 5 and 6 of Table 3.

The increment of this sum has evolved with an average rate of 6.2%; a number close to that of RIS considered alone, given the importance of its load. This sum would have been the synchronous global peak of both RIS and RIN networks if they were interconnected.

The annual peak of the RIN is offset in time from two to three months compared to the RIS. It took place on the same period, twice in the month of February, but most often it occurs in March, a working day by 8PM. This peak has evolved at an average rate of 4.5% per annum. The load synchronous in the RIS with the annual peak of the RIN (same year, same day and same time) was determined and the amount of synchronous MW of the two networks at the forefront of RIN was calculated (see 12 and 13). The Increment of the synchronous sum has evolved at an

average rate of 5.4%. This sum would have been the global synchronous peak of the two RIS and RIN networks during the period from February to March if they were interconnected. Based on the overall load synchronous with the peak of RIS end of previous year (n-1), calculation shows that if the low water period allowed, the power available to the peak of the RIN (February - March) of the year "n" would enable a transfer of power from the RIS to the RIN during the peak of the RIN of the same year. This assignable power is variably carried on from one year to another, between 4.9 MW (2008) and 74.7 MW (2011); Except in 2007 during which the sum of the loads of the two synchronous networks exceeded that obtained at the forefront of December 2006 (three months earlier) in March.

Line 15 of Table 3 presents the sum of the individual non-synchronous peaks of the two networks. The comparison between the non-synchronous sum of the individual peaks (see line 15) to the highest synchronous peak of December (see line 6) gives an expansion coefficient of 0.99. A coefficient of expansion can be considered as the ratio between (i) the sum of synchronous loads of the two networks at the forefront of RIS in a given year and (ii) non-synchronous sum of the two individual peaks of the same year (see line 16 of Table 2.3). This coefficient helps to predict, if the northern and southern networks were interconnected, a global synchronous peak of the two networks by multiplying the sum of the individual peaks of the two networks for the same year by this coefficient.

2.2.4. Duration of use of the Peak at the Central

The calculations were carried out by using the energy produced at each plant the annual peak of the plant. The duration of use calculated for each unit enables to convert the energy produced by a power plant (MWh) into the peak power (in MW).

Table 4. Calculation of the duration of the use of the peak (hours / year) - thermal and hydroelectric power plants connected to the network and isolated plants

Years/ duration of use	2005	2006	2007	2008	2009	2010	2011	Average
Hydro - RIS	6 340	6 258	6 018	6 346	5 968	6 119	6 405	6 208
Hydro- RIN	5 117	5 222	5 229	5 538	5 274	5 447	5 314	5 306
Total Hydro- (RIN + RIS)		6 191	5 967	6 297	5 922	6 075	6 328	6 148
Thermal - RIS	1 226	1 323	2 388	1 474	2 296	2 288	2 582	1 939
Thermal - RIN	*	2	*	5	4	*	*	4
Total Thermal (RIN + RIS)	1 227	1 288	2 388	1 462	2 283	2 288	2 582	1 931
Total (Hydro + Thermal) RIS	5 277	5 261	5 304	5 485	5 240	5 494	5 801	5 409
Total (Hydro + Thermal) RIN	5 120	4 743	5 229	5 390	5 171	5 447	5 314	5 202
Total (Hydro+ Thermal) (RIS+RIN)	5 268	5 231	5 300	5 481	5 237	5 491	5 772	5 397
Totale Isolated Thermal Isolée - RIS	*	*	2 247	3 116	2 836	3 754	3 700	3 131
Totale Isolated Thermal - RIE	*	*	3 918	4 402	4 433	4 223	4 392	4 274
Totale Isolated Thermal- RIN	*	*	3 625	4 374	4 382	4 892	4 688	4 392
Total Isolated Thermal (RIN + RIS+RIE)	*	*	3 586	4 353	4 327	4 467	4 377	4 222
Total Nationwide	5 268	5 231	5 266	5 458	5 218	5 469	5 739	5 379

Source: AES SONEL * Data not shown

Inspection of *Table 4* shows that the life of the hydro is much higher than that of thermal power plants. The overall averages in hours of operation are as follow:

- Hydroelectric power plants: 6,148 h / year (with a higher average for Edea plant i.e 6929 h / year)
- Thermal power stations connected to the network: 1931 h / year
- Hydroelectric power and thermal plants connected: 5397 h / year
- isolated thermal power plants: 3910 h / year
- Global Production (plants only managed by AES SONEL): 5417 h / year

Note that the utilization factor is the life of the peak relative to the number of hours of the year that is 8760 hours.

3. Data Modeling

Two types of data have been used for modeling the demand for electrical energy in Cameroon: meteorological data and monthly electricity peak of RIS and RIN networks.

3.1. Rate of Electricity Coverage in Different Networks

In 2007, the lowest covered region in electricity was the Far North, while the highest coverage rate was recorded in the South. *Figure 5* shows rate of access to electricity and poverty index by region.

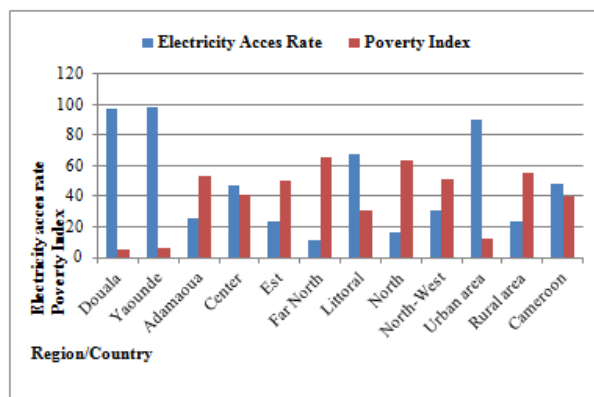


Figure 5. Rate of access to electricity and poverty index by region.

Agglomerations of Yaoundé and Douala have the most beneficial coverage rate. For these regions, this rate of coverage had an average of 48.3% in the same year and proved to be 3.9 times higher in urban than in rural areas. The poorest regions, with the most critical poverty index appeared to be underserved in electrical energy. These regions were: the Great Northern regions (far North and North) and East region. This reflects the social and human issue required for the spatial coverage of the electrical service in these regions. Meteorological parameters used are those of Douala and Ngaoundere respectively for the RIS and INR. When considering the peak power of stations, the most important are located in the Littoral region where the head quarter is Douala. In 2010, it alone concentrated

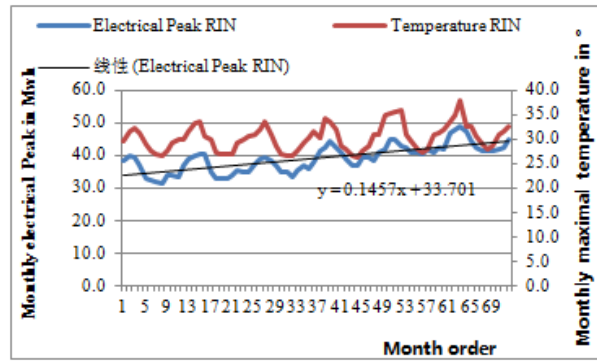
46% of the total peak of RIS. This is due to the fact that Douala is the economic capital; therefore, it has a high concentration of population and industries. According to the statistics of sales of electricity produced by AES SONEL, these two regions consume the greater part of energy of each of the networks. Moreover, the access to electricity is higher in Ngaoundere than in other regions of the RIN. This is why we use meteorological parameters of Douala and Ngaoundere as characteristic for the modeling of the monthly peaks of RIS and RIN respectively.

3.2. The Influence of Meteorological Parameters on the Monthly Peak Electricity Consumption

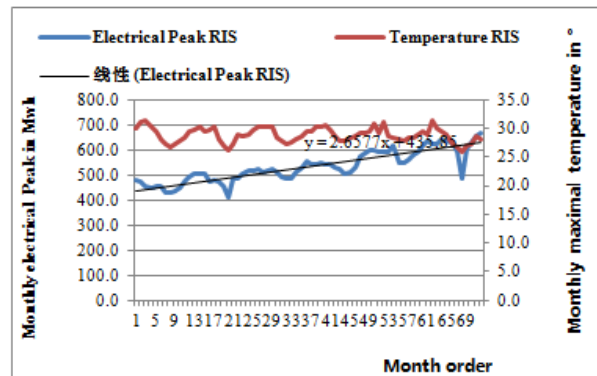
We looked particularly into the maximal temperature, the minimal relative humidity of each month because of their potential influence on the electrical energy consumption. These parameters reflect the interchange of rainy and dry seasons, which are the major climatic events in Cameroon. Meteorological data are obtained from the Meteorological Service of the Ministry of Transport. We did not succeed to obtain the data on the relative humidity in the Ngaoundere (RIN) during the period from 2006 to 2011 because they were not available, thus we only used data from the temperature in this area for modeling.

It has variations on the climate map. A dry season goes from November to February, followed by a short rainy season from March to June, then a big rainy season from August to late September in the South of the country. The average temperature is 26 °C. In the north, the rainy season goes from May to September. The average of the temperature in the Far North is 29 °C; 22 °C in Adamaoua. However, it should be noted that the month of August in the North is the season of heavy rains and the month of March is characterized by high temperatures. In general, thermal amplitudes vary from 7 °C to 40 °C between January and December.

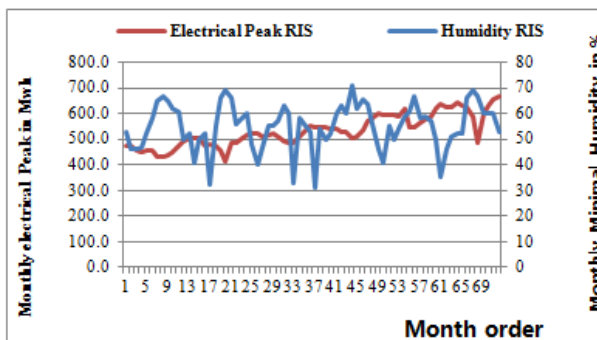
In the area of RIS, we have the following regions with their latitude and longitude: Yaoundé (3° 52' N 11° 32' E, Centre), Douala (04°00'N, 09°45'E., the Littoral), Bafoussam (5°28'N, 10°25'E in the West), Buea (4°09'09" N, 9°14'27" E, South West), Bamenda (5°56' N, 10°1'E North West), Bertoua (4.58333N ,13.6833E, in the East), Bamenda (8 ° 59'N , 1 ° 09'E, North West), South}. In the area of RIN, we have the following regions with their longitude and latitude: (Maroua (10 ° 50'14 .28 "N, 14 ° 55'24 .39" E., in the extreme south), Garoua (9°18'00" N, 13°24'00" E, North), Ngaoundere (13°35'7.19"E, 7°12'33.35"N, in the Adamawa). We use in this paper the data measured in Douala for RIS and in Ngaoundere for RIN.



(a)



(b)



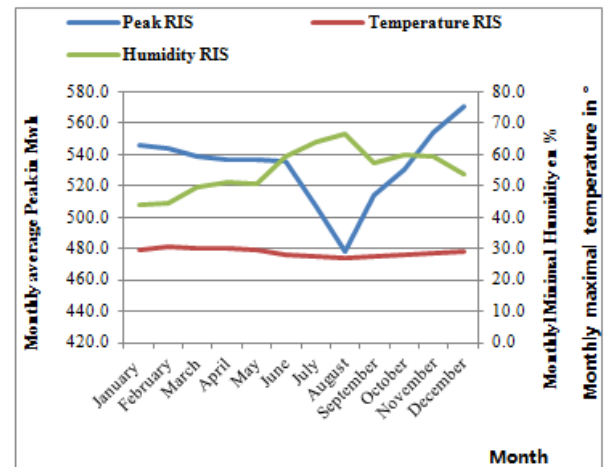
(c)

Figure 6. Evolution of the monthly peak power, maximal and minimal temperature and relative humidity in the RIS and the RIN Networks.

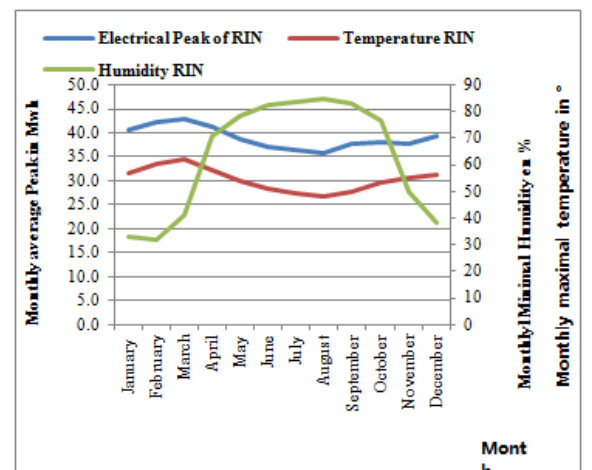
Figure 6. shows the evolution of monthly values of relative humidity and temperature in Douala and Ngaoundere from January 2006 to December 2011. Abscissa, the number 1 is the first month of our data base (January 2006 = 1, February 2006 = 2, December 2011 = 72). The overall observation of this figure shows a high level of humidity of above 57% in the RIS. The temperatures below this threshold reflect the impact of the dry season. It is also observed at the same instants the maximum temperatures of above 28 ° and 32 ° respectively in the RIS and RIN reflecting the effect of the dry season too.

For this study, our sample consists of 72 measures (12 measures per year for six years). The evolution of electric power in Cameroon, reported in Figure 3.2 shows an

increasing trend in the average electricity consumption, added to annual quasi-periodic features. The extrapolation of a linear trend used to evaluate the annual growth rate of energy consumption to about 7%.



(a)



(b)

Figure 7. Profiles normalized peak power, temperature and humidity for the RIS and RIN

Meteorological data, like electrical data peak present seasonal patterns. So there are annual profiles of the electrical peak and profiles of meteorological parameters variations. In Figure 7, normalized profiles of monthly electrical peak, of temperature and humidity are presented. It makes us distinguish the following main properties:

- The existence of electrical peaks during the month N° 2 and 3 in the RIN and N°12 in the RIS (February and March in RIN and December in RIS).
- The existence of a minimum of electrical consumption during the month No. 8 (August) for RIS and RIN.
- The maximum of electrical consumption corresponds to the maximum of temperature
- The temperature variations are in phase opposition with the relative humidity.
- The annual electrical peak corresponds to the

maximum of temperature and the minimum of humidity. These moments are representative of the dry season, more adequate to a high electrical consumption.

4. Methodology

4.1. General

A time series is a set of observations that are distinguished by the important role that the order in which they were collected plays. The principal models for the study of time series are:

- Autoregressive models ("Auto - Regressive").

They were introduced by Yule [24]. In these models, we take into account a linear dependence of the process of its own lag.

$$X_t = \alpha_1 X_{t-1} + \alpha_2 X_{t-2} + \dots + \alpha_p X_{t-p} + u_t$$

Where $p \in \mathbb{N}^*$ is the order of the process, $\alpha_1, \alpha_2, \dots, \alpha_p$ are real constants and $(u_t)_{t \in \mathbb{Z}}$ is white noise.

- Moving average models («Moving Average»)
- They were introduced by Slutsky [24]. A moving average process is the sum of white noise and its past:

$$MA(q) : X_t = u_t + \beta_1 u_{t-1} + \beta_2 u_{t-2} + \dots + \beta_p u_{t-q}$$

Where $q \in \mathbb{N}^*$ and $\beta_1, \beta_2, \dots, \beta_p$ are real constants.

- ARMA models ("Auto - Regressive Moving Average")
- Developed by Box & Jenkins [Box & Jenkins, 1970]. ARMA models are a combination of autoregressive and moving average models:

$$ARMA(p, q) : X_t - \alpha_1 X_{t-1} - \alpha_2 X_{t-2} - \dots - \alpha_p X_{t-p} = u_t + \beta_1 u_{t-1} + \beta_2 u_{t-2} + \dots + \beta_p u_{t-q}$$

- The ARIMA (Autoregressive Integrated Moving Average) and SARIMA (Seasonal Autoregressive Integrated Moving Average) (a SARIMA process is an integrated ARMA process with seasonal component) [Box & Jenkins in, 1970].

ARIMA and SARIMA models were then developed in order to model a large number of real phenomena that present trends and / or seasonality. ARMA models are applied to integrated series.

Linear regression is a statistical technique used to model the linear relationship between exogenous variables (denoted Y_{it}) and an endogenous variable (denoted by X_t).

$$X_t = \alpha_0 + \alpha_1 X_{t-1} + \alpha_2 Y_{1t} + \alpha_3 Y_{2t} + \dots + \alpha_n Y_{nt} + u_t$$

Where:

- X_t Is the variable to be explained in our article, which is monthly electrical peak
- X_{t-1} is the lag value for the monthly electrical peak
- Y_{it} The exogenous variables (temperature (T), relative humidity (H), Order of the month (M))

$\alpha_0, \alpha_1, \dots, \alpha_n$ are the parameters to estimate from the model.

u_t is the white noise defined by the relation :

$$u_t = \beta_1 u_{t-1} + \beta_2 u_{t-2} + \dots + \beta_p u_{t-p} + \varepsilon_t$$

Reference [4] recommends the use of seasonal autoregressive (SAR) and seasonal moving average (SMA) terms for monthly data with systematic seasonal movements. A SAR (p) term can be included in our equation specification for a seasonal autoregressive term with lag p. The lag polynomial used in estimation is the product of the one specified by the AR terms and the one specified by the SAR terms. The purpose of the SAR is to allow you to form the product of lag polynomials.

Similarly, SMA (q) can be included in our specification to specify a seasonal moving average term with lag q. The lag polynomial used in estimation is the product of the one defined by the MA terms and the one specified by the SMA terms. As with the SAR, the SMA term allows you to build up a polynomial that is the product of underlying lag polynomials.

Modeling power of monthly electrical peak of RIS and RIN, made by a SARIMA model is expressed in terms of the order of months, the maximal temperature and the minimal relative humidity and the terms of seasonality as well.

4.2. Models for RIS

The models used for modeling the monthly electrical peak of the Interconnected South (RIS) network are:

$$C_{t1} = \alpha_0 + \alpha_1 T_t + \alpha_2 H_t + \alpha_3 M_t + u_t \quad (1)$$

$$C_{t2} = \alpha_0 + \alpha_1 T_t + \alpha_2 H_t + \alpha_3 M_t + \alpha_6 C_i + u_t \quad (2)$$

$$\ln(C_{t3}) = \alpha_0 + \alpha_1 T_t + \alpha_2 H_t + u_t \quad (3)$$

$$\ln(C_{t4}) = \alpha_0 + \alpha_1 T_t + \alpha_2 H_t + \alpha_3 M_t + u_t \quad (4)$$

$$\ln(C_{t5}) = \alpha_0 + \alpha_2 H_t + \alpha_3 M_t + u_t \quad (5)$$

$$\ln(C_{t6}) = \alpha_0 + u_t \quad (6)$$

$$\ln(C_{t7}) = \alpha_0 + \alpha_1 T_t + \alpha_2 H_t + \alpha_3 M_t + \alpha_6 C_i + u_t \quad (7)$$

Where:

T_t is the temperature at month t.

H_t is the relative humidity at month t.

M_t is the order of the month (1 = January 2006 December 2006 = 12, 13 = January 2007 = 24 December 2007).

C_i is the average seasonal coefficient for each month.

u_t is white noise.

Where α_0 and $(\alpha_1, \alpha_2, \alpha_3, \alpha_4, \alpha_5, \alpha_6, \alpha_7)$ are intercepted and regression coefficients, respectively. For handling serial correlation, we implement autoregressive in the error term of demand models. This usual method is expressed in equation (8). Here, autoregressive order two model is applied in the composed regression models. As options, models without and with autoregressive model of order one are computed as well.

$$u_t = \beta_1 u_{t-1} + \beta_2 u_{t-2} + \dots + \beta_p u_{t-p} + \varepsilon_t = \beta_1 sma(12) + \beta_2 sar(12) + \varepsilon_t \quad (8)$$

Where u_t , β_p and p are ε_t error term, constant, autoregressive order, and a white noise, respectively. (*sar(12)*) and (*sma(12)*) are seasonal autoregressive and seasonal moving average terms for monthly respectively.

4.3. Models for RIN

The models used for modeling the monthly peak of North interconnected network (RIN) are:

$$C_{t1'} = \alpha_0 + \alpha_1 T_t + \alpha_2 H_t + \alpha_3 M_t + \alpha_4 M_t^2 + u_t \quad (1')$$

$$C_{t2'} = \alpha_0 + \alpha_1 T_t + \alpha_2 H_t + \alpha_3 M_t + \alpha_4 M_t^2 + \alpha_5 M_t^3 + \alpha_6 C_i + u_t \quad (2')$$

$$\ln(C_{t3'}) = \alpha_0 + \alpha_1 T_t + \alpha_2 H_t + u_t \quad (3')$$

$$\ln(C_{t4'}) = \alpha_0 + \alpha_2 T_t + \alpha_3 M_t + \alpha_4 M_t^2 + u_t \quad (4')$$

$$\ln(C_{t5'}) = \alpha_0 + \alpha_3 M_t + \alpha_4 M_t^2 + u_t \quad (5')$$

$$\ln(C_{t6'}) = \alpha_0 + u_t \quad (6')$$

$$\ln(C_{t7'}) = \alpha_0 + \alpha_1 T_t + \alpha_2 H_t + \alpha_3 M_t + \alpha_4 M_t^2 + \alpha_5 M_t^3 + \alpha_6 C_i + u_t \quad (7')$$

Where α_0 and ($\alpha_1, \alpha_2, \alpha_3, \alpha_4, \alpha_5, \alpha_6, \alpha_7$) are intercepted and regression coefficients, respectively. For handling serial correlation, we implement autoregressive in the error term of demand models. This usual method is expressed in equation (8'). Here, autoregressive order two model is applied in the composed regression models. As options, models without and with autoregressive model of order one are computed as well.

$$u_t = \beta_1 u_{t-1} + \beta_2 u_{t-2} + \dots + \beta_p u_{t-p} + \varepsilon_t = \beta_1 \text{sma}(12) + \beta_2 \text{sar}(12) + \varepsilon_t \quad (8')$$

Where u_t , β_p and p are ε_t error term, constant, autoregressive order, and a white noise, respectively. (*sar(12)*) and (*sma(12)*) are seasonal autoregressive and seasonal moving average terms for monthly respectively.

5. Results

Table 5. Results of ADF and PP tests

variable	Differentiation of order 0		Differentiation of order 1		Résultats
	p-value PP.test	p-value ADF.test	p-value PP.test	p-value ADF.test	
PRIS	0.6665	0.9940	0.0000	0.0000	d =1
Ln (PRIS)	0.7657	0.7147	0.0000	0.0000	d =1
TRIS	0.0001	0.0001	*	*	d =0
HRIS	0.0001	0.0001	*	*	d =0
PRIN	0.2572	0.9896	0.0000	0.0000	d=1
LN(PRIN)	0.2551	0.9787	0.0000	0.0000	d=1
TRIN	0.0108	0.9725	*	*	d=0

Table 6. Regression coefficients for RIS

Explanation Variable	Model 1		Model 2		Model 3		Model 4	
	Coef.	Prob. (p-value)	Coef.	Prob. (p-value)	Coef.	Prob. (p-value)	Coef.	Prob. (p-value)
T_t	0.3244	0.9154	1.0178	0.5935	-0.003	0.5654	0.0019	0.7233
	-3.0409	0.10670*	-1.895	0.5369*	-0.0052	-0.578*	-0.0053	0.3558*
H_t	0.0958	0.7074	0.2479	0.2609	0.0002	0.5146	0.0002	0.5376
	-0.2541	0.3773*	-0.218	1.1364*	-0.0004	0.6558*	-0.0004	0.6204*
M_t	36.4687	0.8307	3.20944	0			0.016	0.4012
	-169.768	0.2148*	-0.21	15.2391*			-0.019	0.8461*
SMA(12)	-0.86034	0	-0.8569	0	-0.8815	0	-0.8729	0
	-0.0348	-24.700*	-0.052	-16.298*	-0.0375	-23.45*	-0.0361	-24.14*
SAR(12)	0.9902	0	0.3558	0.0355	0.9997	0	0.9706	0
	-0.0484	20.4274*	-0.164	2.1579*	-0.0312	31.997*	-0.0454	21.375*
α_0	-42031.82	0.9205	-170.79	0.0122	251.479	0.9932	1.2211	0.9355
	-419120	-0.1002*	-65.8	-2.5955*	-29512	0.0085*	-15.03	0.0812*
C_i			-535.3	0				
			-53.29	10.0461*				

Table 6 continued

Explanation Variable	Model 5		Model 6		Model 7	
	Coef.	Prob. (p-value)	Coef.	Prob. (p-value)	Coef.	Prob. (p-value)
T_t						
H_t	0.00026	0.5565			0.0004	0.1586
M_t	-0.0004	0.5916*			-0.0003	1.4297*
	0.0153	0.3838			0.0054	0
	-0.0174	0.8780*			-0.0002	27.0843*
SMA(12)	-0.8729	0	-0.8807	0	-0.8596	0
	-0.036	-24.22*	-0.036	-24.16*	-0.0476	-18.031*
SAR(12)	0.9718	0	0.9998	0	0.2444	0.1028
	-0.0433	22.425*	-0.028	35.452*	-0.1472	1.6594*
α_0	1.4342	0.9213	373.06	0.995	5.0819	0
	-14.442	0.0993*	-59237	0.0062*	-0.0764	66.5018*
C_i					0.9603	0
					-0.0613	15.662*

() T-statistic, * adj. standard error, _ the related variable is not significant.

To determine the most appropriate model for our study, we firstly performed stationary tests (Augmented Dickey-Fuller (ADF) and Phillips-Perron (PP)) on the variables used. From these tests, we find that the meteorological variables (temperature and relative humidity) are stationary while the variable electrical peak is integrated at order 1. Results of these tests are recorded in Table 5. So, we can apply the model of linear regression over time.

The different models used are those minimizing the Akaike (AIC) and Schwartz (SC) criteria. Tests Fisher and Student tests which are respectively global and individual significance of coefficients of various parameters are listed

in Tables 6 and 7. From the analysis of the coefficients of the parameters, we can see that the coefficients of meteorological parameters are not significant because the p-value of these variables are greater than the threshold $\alpha = 5\%$.

After having removed these variables, we find that AIC and SC increases, meanwhile the best models are based on AIC and SC weak. Conclusively, we can say that the coefficients related to the temperature and the relative humidity is significant for our different models. Meteorological parameters thus influence the monthly peak C_t .

Table 7. Regression statistics of RIS

Linear Models	R^2	$R^{2'}$	SE Reg.	Prob. (F-Stat)	AIC	SC	White-test		JB-test (p-value)	F-Stat	B-D (LM) D-W	
							ORS (p-value)	F-stat (p-value)			ORS (p-value)	F-stat (p-value)
Model 1 (C_{t1})	0.9576	0.9537	11.9938	0.0000	7.9013	8.1107	22.7978 (0.5894)	0.8334 (0.6784)	8.4332 (0.0147)	244.2695	3.0302 (0.5528)	0.6759 (0.6118)
Model 2 (C_{t2})	0.9708	0.9675	10.0385	0.0000	7.5600	7.8043	42.4642 (0.1803)	1.6605 (0.0984)	0.4018 (0.8179)	294.5922	1.8593 (0.7616)	0.5172 (0.7234)
Model 3 ($\ln(C_{t3})$)	0.9576	0.9545	0.0215	0.0000	-4.7541	-4.579	11.8734 (0.8910)	0.5193 (0.9368)	5.0115 (0.081)	310.7885	1.8063 (0.7713)	0.5383 (0.7082)
Model 4 ($\ln(C_{t4})$)	0.9601	0.9564	0.0211	0.0000	-4.7812	-4.571	23.1823 (0.6752)	0.7462 (0.7794)	5.5480 (0.0624)	259.9912	1.5936 (0.8099)	0.3638 (0.8332)
Model 5 ($\ln(C_{t5})$)	0.9600	0.9571	0.0209	0.0000	-4.8122	-4.637	16.8179 (0.6648)	0.7594 (0.7415)	5.7856 (0.0554)	330.2031	1.5774 (0.8128)	0.3592 (0.8364)
Model 6 ($\ln(C_{t6})$)	0.9568	0.9553	0.0213	0.0000	-4.8029	-4.698	6.1170 (0.6341)	0.7237 (0.6698)	4.2694 (0.1182)	632.2619	1.6126 (0.8065)	0.5974 (0.6661)
Model 7 ($\ln(C_{t7})$)	0.9743	0.9719	0.0169	0.0000	-5.2209	-5.011	32.0468 (0.2304)	1.3587 (0.2019)	0.0738 (0.9637)	409.5155	1.1812 (0.8812)	0.2710 (0.8953)

() P-value

The coefficients of determination of the models of RIS and RIN are between (0.953 and 0.971) and (0.944 and 0.971) respectively and Prob (F-stat) is zero for these models. We can therefore conclude that our models are valid. We can also note that the application of the variable logarithm C_t allows us to have an AIC and a SC even

lower. The introduction of seasonal coefficient C_i allows us to have the best model for both networks.

For RIS model, we have following graphs : (B) forecast series in blue and forecast intervals to 95% in red (A) observation series in red, forecast series in green and residue in blue) ;

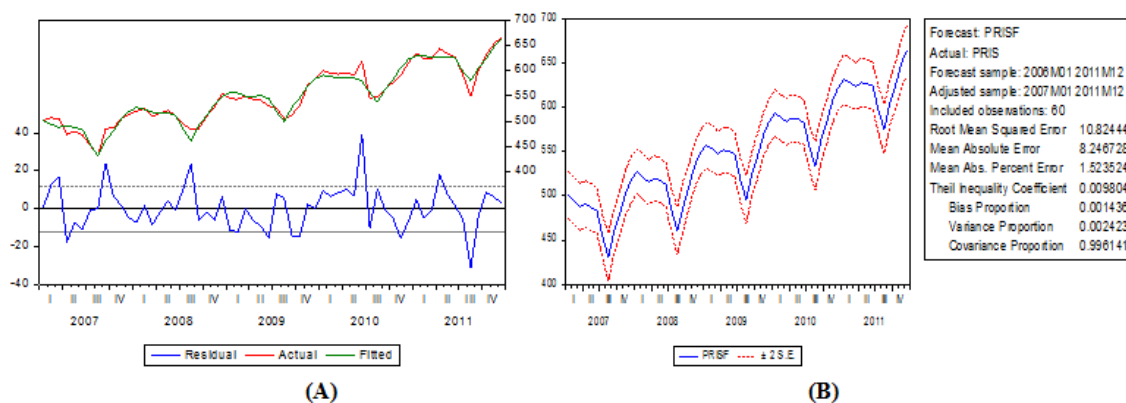


Figure 8. Model 1

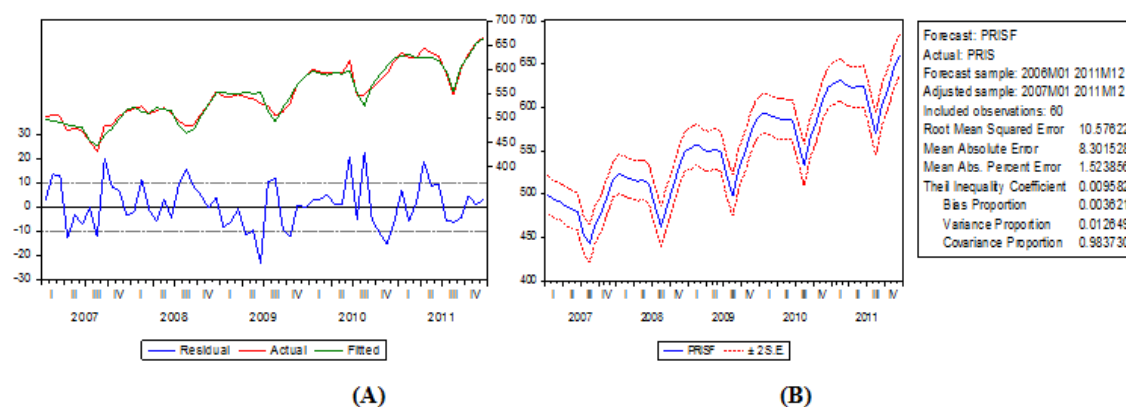


Figure 9. Model 2

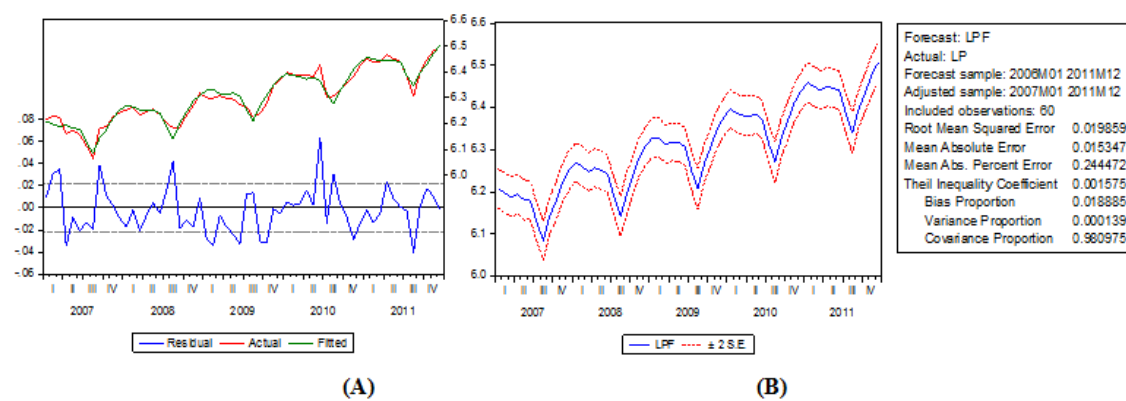


Figure 10. Model 3

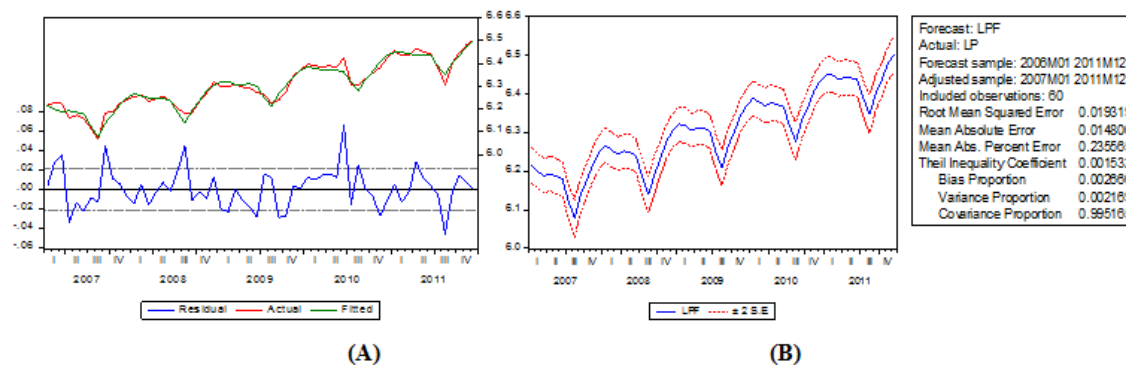


Figure 11. Model 4

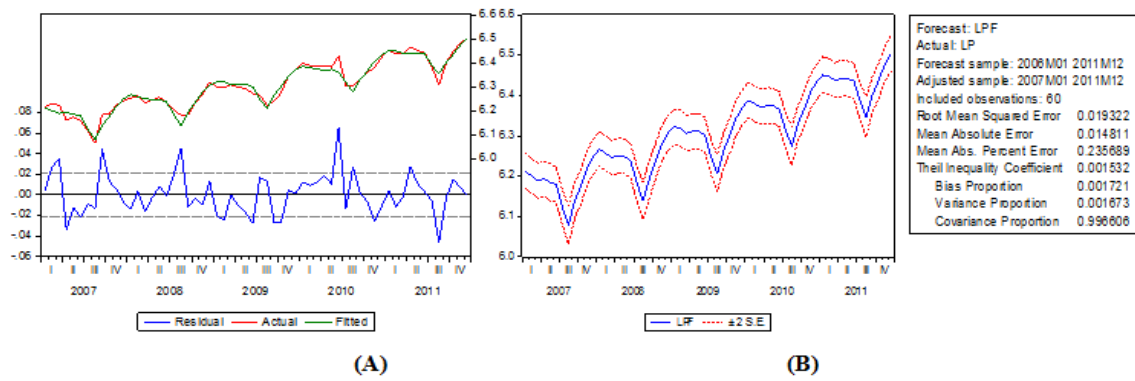


Figure 12. Model 5

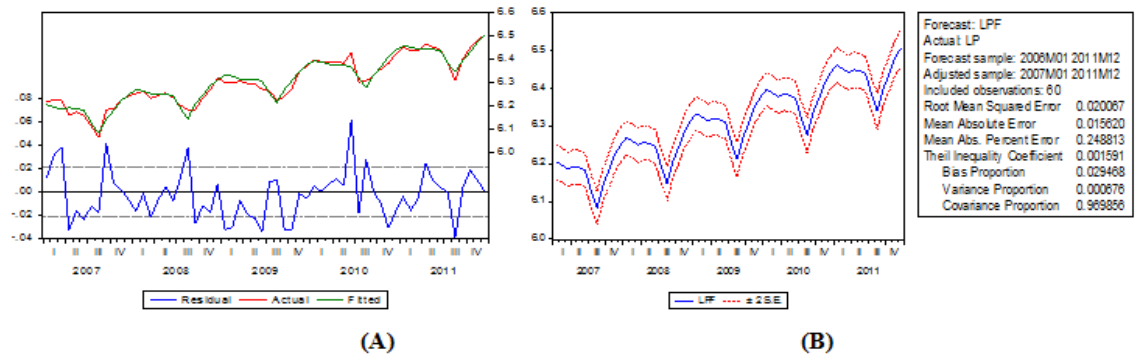


Figure 13. Model 6

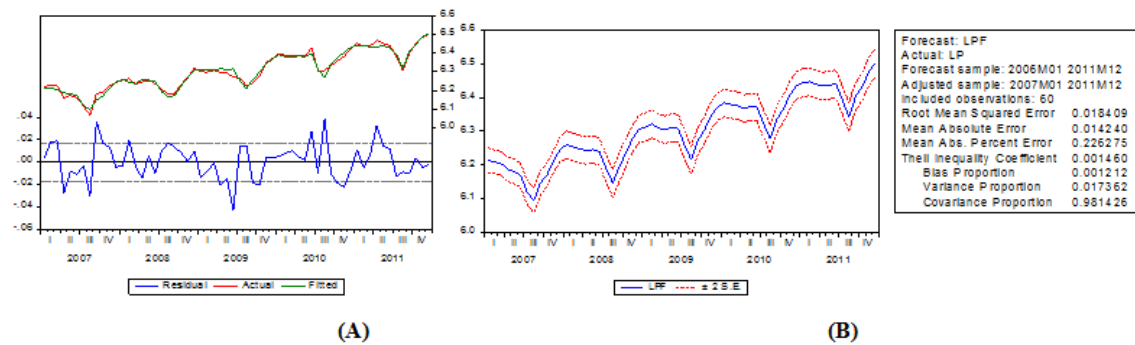


Figure 14. Model 7

Table 8. Regression coefficients for RIN

Explanation Variable	Model 1'		Model 2'		Model 3'		Model 4'	
	Coef.	Prob.(p-value)	Coef.	Prob.(p-value)	Coef.	Prob.(p-value)	Coef.	Prob.(p-value)
T_t	-0.2333	0.0911	-0.1382	0.0859	-0.0057	0.0708	-0.00595	0.0817
	-0.1355	-1.721*	-0.0781	-1.752*	-0.0031	-1.843*	-0.0033	-1.7755*
M_t	27.6491	0.5284	-0.5636	0.0883			0.430044	0.3573
	-43.557	0.6347*	-0.3241	-1.7386*			-0.463	0.9287*
M_t^2	-0.0546	0.2932	0.0195	0.0101			-0.0011	0.1507
	-0.0514	-1.061*	-0.0073	2.6735*			-0.0007	-1.458*
M_t^3			-0.0001	0.0052				
			-5.22E-05	-2.9216*				
SMA(12)	-0.8567	0	-0.8628	0	-0.8816	0	-0.8748	0
	-0.0404	-21.16*	-0.0422	-20.413*	-0.0345	-25.55*	-0.0388	-22.51*
SAR(12)	0.9439	0	0.07307	0.6039	0.9296	0	0.9234	0
	-0.0454	20.746*	-0.1399	0.52207*	-0.0472	19.666*	-0.0423	21.827*
AR(1)	0.4389	0.0021	0.17491	0.242	0.6185	0	0.3985	0.0057
	-0.1352	3.2453*	-0.1477	1.18411*	-0.103	5.987*	-0.1383	2.880*
α_0	-5760.9	0.6777	3.10168	0.5219	4.7285	0	-62.1448	0.5609
	-13783	-0.417*	-4.8094	0.6449*	-0.666	7.099*	-106.181	-0.585*
C_i			40.6466	0				
			-3.3255	12.2225*				

Table 8. continued

Explanation Variable	Model 5'		Model 6'		Model 7'	
	Coef.	Prob.(p-value)	Coef.	Prob.(p-value)	Coef.	Prob.(p-value)
T_t					-0.0038	0.0831
					-0.0021	-1.7681*
M_t	0.16109	0.1611			-0.01415	0.1908
	-0.1133	1.4212*			-0.0106	-1.3261*
M_t^2	-0.0006	0.0648			0.00048	0.0396
	-0.0003	-1.885*			-0.0002	2.1133*
M_t^3					-3.72E-06	0.0215
					-1.50E-06	-2.3742*
SMA(12)	0.1409	0	-0.892	0	-0.88211	0
	-2.6045	2.6045*	0.03549	-25.134	-0.0374	-23.577*
SAR(12)	0.8712	0	0.88485	0	0.1717	0.1638
	-0.0453	19.209*	0.05184	17.0662	-0.1215	1.4130*
AR(1)	0.36702	0.0119	0.58696	0	0.21152	0.168
	-0.1409	2.6045*	0.10831	5.41891	-0.1511	1.3990*
α_0	-11.066	0.4605	4.17269	0	2.80242	0
	-14.885	-0.743*	0.23605	17.6765	-0.16911	16.5710*
C_i					0.99491	0
					-0.0922	10.7894*

() t-statistic, *ajds. standard error, _ the related variable is not significant

To verify the absence of autocorrelation of residues for the different models, we conducted the Breusch-Godfrey test (BG) on all models because in these models we have use endogenous variable delayed among the exogenous variables by introducing the terms SMA (12) and SAR (12). Residues are correlated with the threshold $\alpha = 5\%$ if P-value < 0.05 . The analysis of test BG to order 4 and the threshold $\alpha = 5\%$, shows that P-value > 0.05 for all models. We can therefore accept the hypothesis of no autocorrelation of residues for all models. The test of White (1980) applied to these models allow us to accept the hypothesis of no heteroscedasticity of errors for, the threshold $\alpha = 5\%$, P-value > 0.05 . Our residue being homoscedastic it is a white noise. The results of these tests

are listed in *Tables 8 and 9*.

To know whether our white noise is Gaussian, we performed the Jarque-Bera test (JB). The hypothesis of obtaining a Gaussian white noise is true at the threshold $\alpha = 5\%$, if the Jarque-Bera statistic is greater than the one read from the table of chi-square (JB stat < 5.99) and the probability of the Jarque-Bera statistic provided by Eviews is below the defined threshold (P-value $> 5\%$). The analysis of this test allows us to accept the hypothesis of a Gaussian white noise for all models except Model 1 not which does not fulfilled the conditions of Gaussian white noise because JB stat = 8.4332 > 5.99 and P-value = 0.0147 < 0.05 . The results of the various tests are listed in *Tables 8 and 9*.

Table 9. Regression statistics of RIN

Linear Models	R^2	R^{2*}	SE Reg.	Prob. (F-Stat)	AIC	SC	White-test		JB-test (p-value)	F -Stat	B-D (LM) D-W	
							ORS (p-value)	F-stat (p-value)			ORS (p-value)	F- stat (p-value)
Model 1' (C_{t1}')	0.9503	0.9446	0.9290	0.0000	2.8017	3.0482	34.0937 (0.3672)	1.1122 (0.394)	0.4474 (0.7996)	166.026	3.24199 (0.5182)	0.69939 (0.5962)
Model 2 (C_{t2}')	0.9744	0.9703	0.6804	0.0000	2.2073	2.52429	54.7319 (0.4086)	1.2097 (0.4635)	1.6930 (0.4289)	238.034	2.461882 (0.6515)	0.500755 (0.7353)
Model 3' ($\ln(C_{t3}')$)	0.9499	0.9461	0.0231	0.0000	-	-	17.1471 (0.6434)	0.7784 (0.721)	0.5353 (0.7651)	255.959	-	0.55424 (0.6968)
Model 4' ($\ln(C_{t4}')$)	0.9547	0.9495	0.0224	0.0000	-	-	32.0447 (0.4645)	0.9659 (0.5418)	0.7031 (0.7035)	182.8579	1.46804 (0.8323)	0.30679 (0.8720)
Model 5' ($\ln(C_{t5}')$)	0.9526	0.9481	0.0227	0.0000	-	-	36.1437 (0.0891)	1.9462 (0.0371)	1.2144 (0.5448)	213.2253	2.53024 (0.6392)	0.54889 (0.7007)
Model 6' ($\ln(C_{t6}')$)	0.9473	0.9444	0.0235	0.0000	-	-	15.78257 (0.3268)	1.1477 (0.3470)	0.7154 (0.6992)	176.3218	0.7129 (0.9497)	0.6889 (0.6030)
Model 7' ($\ln(C_{t7}')$)	0.9754	0.9715	0.0168	0.0000	-	-	56.3379 (0.3512)	1.9965 (0.2258)	1.2724 (0.5290)	248.3225	1.75405 (0.7809)	0.35392 (0.8400)

() p-value

For RIN model, we have the following graphs : (B) observation series in red, forecast series in green and forecast intervals to 95% in red (A) observation series in red, forecast series in green and residue in blue ;

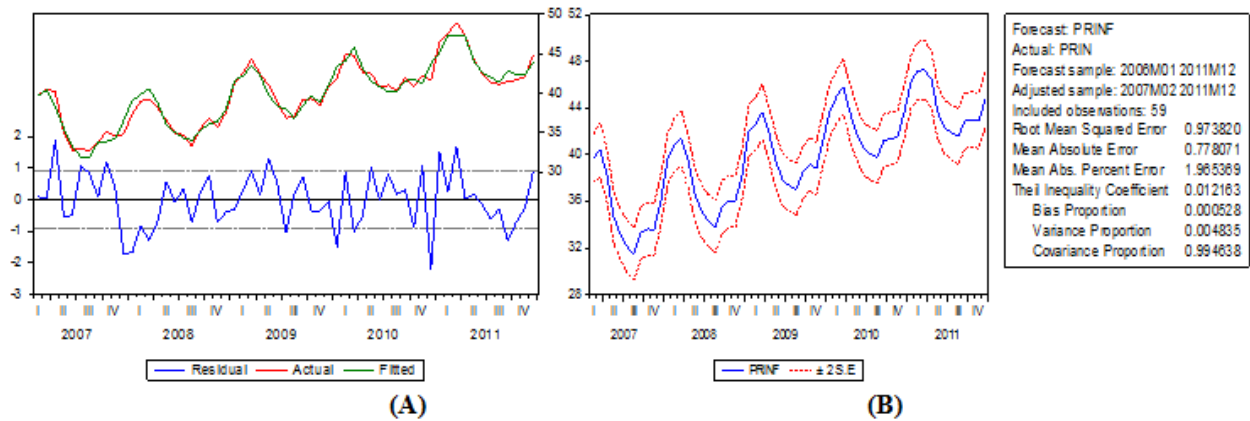


Figure 15. Model 1'

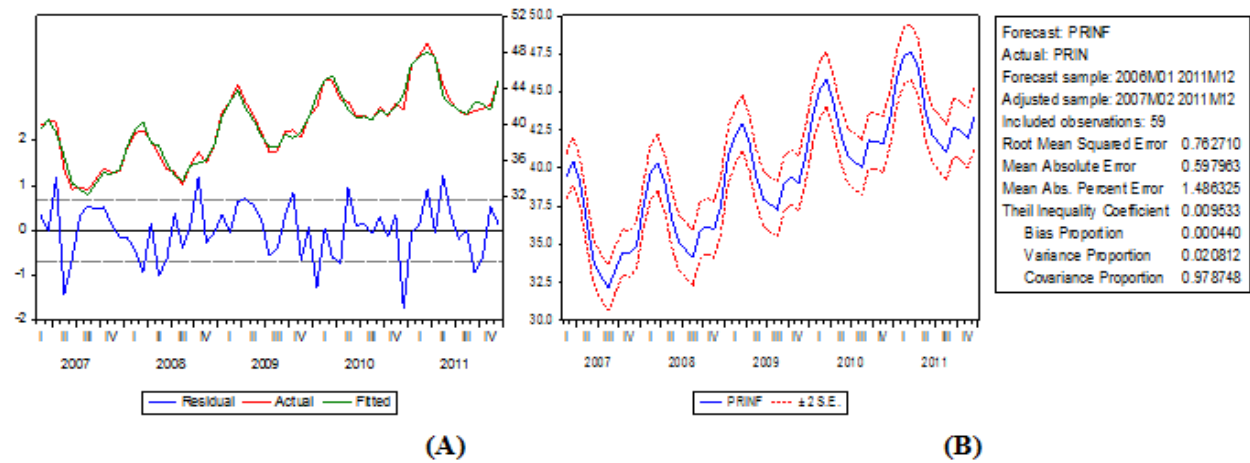


Figure 16. Model 2'

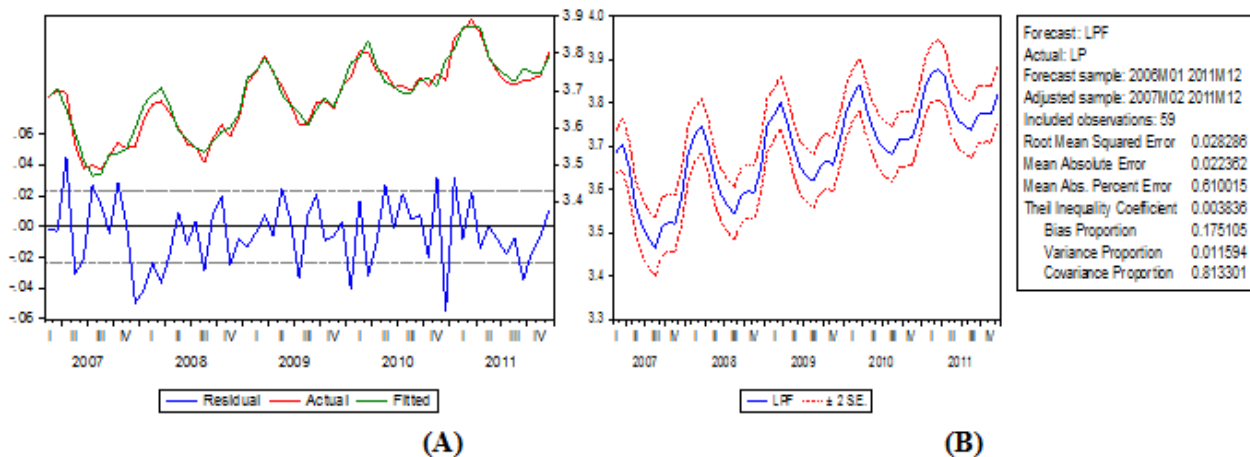


Figure 17. Model 3'

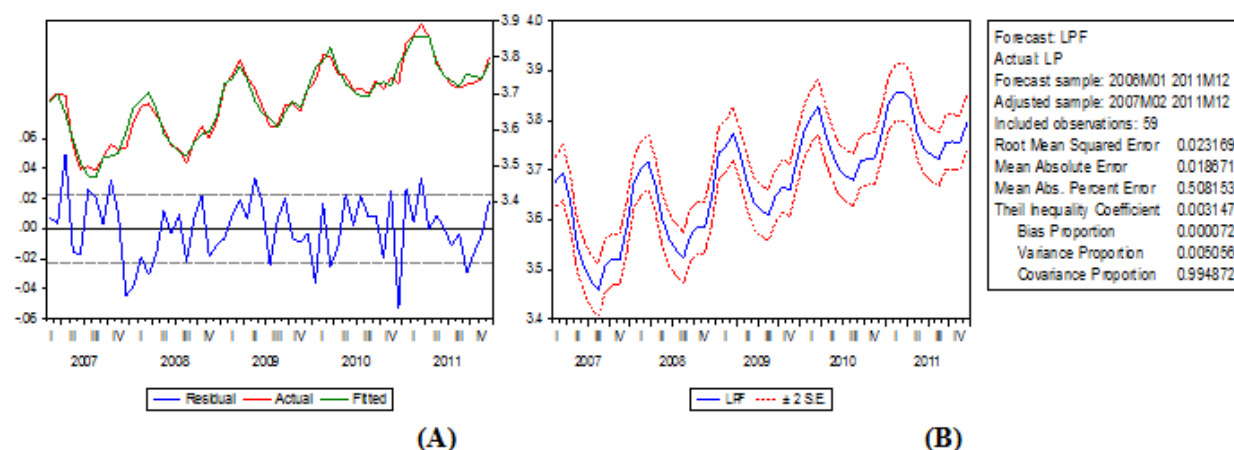


Figure 18. Model 4'

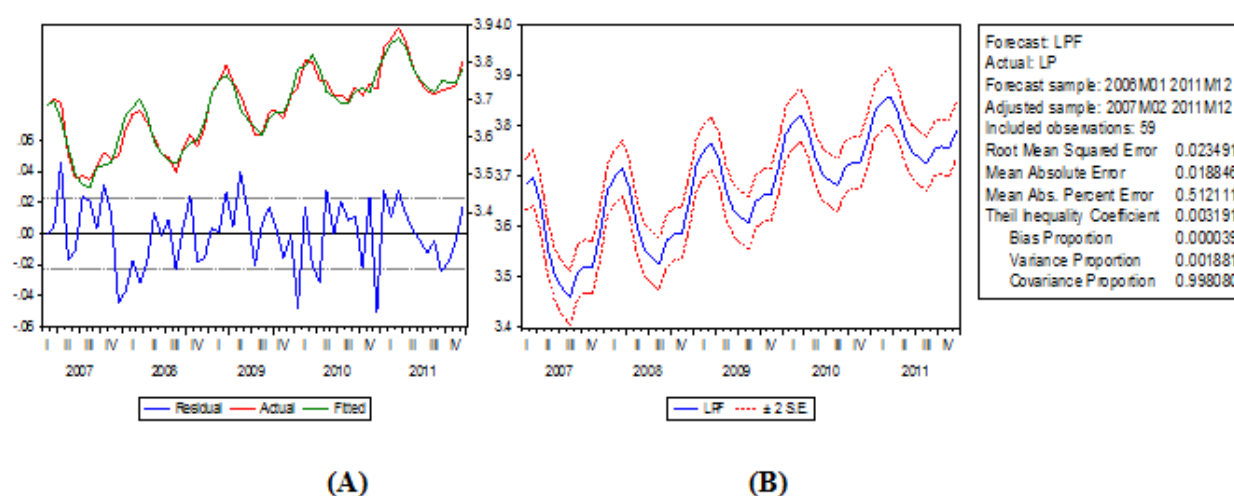


Figure 19. Model 5'

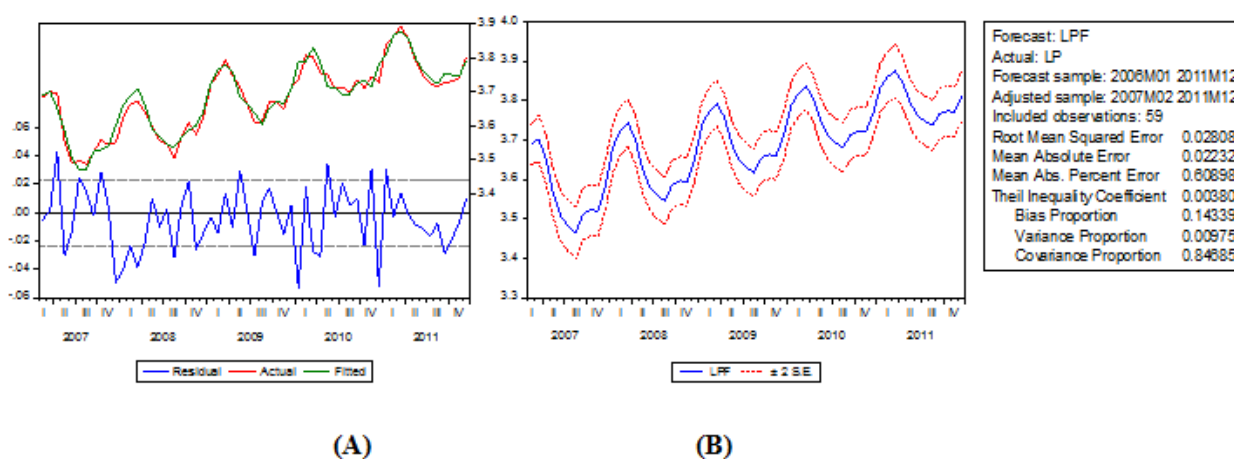


Figure 20. Model 6'

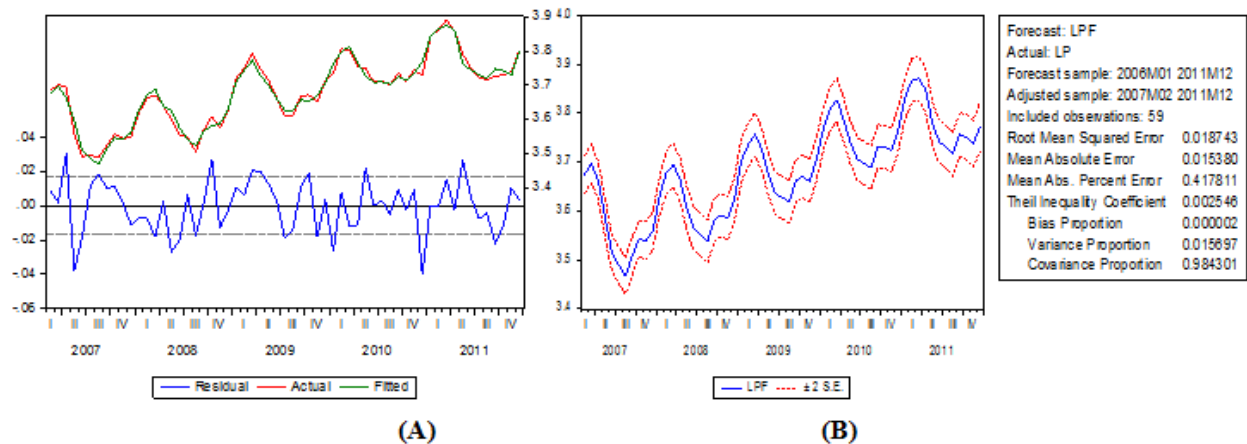


Figure 21. Model 7'

6. Conclusion and Comments

This study presents the modeling of the electricity monthly peak consumption of the main interconnected Cameroon namely the interconnected South (RIS) and North (RIN), using econometric techniques notably linear regression model networks. Meteorological parameters are considered as explanatory variables. We also noted that the application of the logarithm to the variable allows us to have an AIC and an even lower SC. The introduction of seasonal coefficient c_i allows us to have the best model for both networks.

With the coming of this analysis, we note that meteorological parameters play a key role in the electricity monthly peak consumption in Cameroon. This is justified by the maxima and minima observed respectively in the dry and rainy season in both networks. Although the two areas do not have the same climate, the minimum of electricity monthly peak is observed during the month of August which is the wettest month in the country and also the month of holidays in several companies. The maximum observed in December for the RIS, this can be justified by the use of air conditioners and fans because of the heat caused by the onset of the dry season, but especially the preparations for the Christmas party and end year ceremonies. It should be noted that much of the population in the RIS area is Christian, so it gives a particular importance to the Christmas party. The use of garlands and bright decorations could also justify the high demand during this period. The strong demand of electricity in the RIS area can also be justified by the presence of political capital (Yaoundé) and economic (Douala) in this area. Large industries, departments and universities are also grouped in the majority in this area. December being the last month of the year and the month of heavy consumption of products; many companies increase their production to meet the high demand for this period. The closure of the financial year being also done in December, several companies must take stocks and develop strategies for the New Year. This requires extra works days or hours. This causes an increase in hours of work and resources leading

to the use of additional electricity period consumption.

In the RIN, the electricity monthly peak consumption is generally observed in March and February. These two months correspond to the warmest months in this area. Refrigerators, freezers, Fans and air conditioners are stretched to their highest capacities because of the sweltering heat during this period. We also notice that the coefficients related to seasonality are highly significant in all models. This is due to climate variations that make the electrical monthly peak to be seasonal.

Acknowledgements

The authors thank Demsong Bethin for his help in the translation. We would like to express our sincere gratitude to the anonymous reviewers and the Editor of the Journal for many valuable comments.

References

- [1] AES - SONEL, 2011 Rapport AES/AREVA.
- [2] Annuaire statistique 2010 du Cameroun – INS et Document de Stratégie pour la Croissance et l'Emploi- Rapport Définitif – Août 2009.
- [3] A. Pardo, V. Meneu and E. Valor, "Temperature and Seasonality Influences on Spanish Electricity Load," Energy Economics, Vol. 24, pp. 55-70, 2002.
- [4] Box, George E. P. and Gwilym M. Jenkins (1976). Time Series Analysis: Forecasting and Control, Revised Edition, Oakland, CA: Holden-Day.
- [5] C. Adjamagbo, P. Ngae, A. Vianouet V. Vigneron « Modélisation de la demande en énergie électrique au Togo » Revue des Energies Renouvelables Vol. 14 N°1 (2011) 67 – 67.
- [6] Context of Auto-Correlated Errors," Journal of the American Statistical Association, 64, 253–272.
- [7] D. H. W. Li, J. C. Lam, and S. L. Wong, "Daylighting and Its Effects on Peak Load Determination," Energy, Vol. 30, pp. 1817-1831, 2005.

- [8] EViews. <http://www.eviews.com>
- [9] Fair, Ray C. (1984). *Specification, Estimation, and Analysis of Macroeconometric Models*, Cambridge, MA: Harvard University Press.
- [10] F. Egelioglu, A. A. Mohamad, and H. Guven, "Economic Variables and Electricity Consumption in Northern Cyprus," *Energy*, Vol. 26, pp. 355-362, 2001.
- [11] Greene, William H. (2008). *Econometric Analysis*, 6th Edition, Upper Saddle River, NJ: Prentice-Hall.
- [12] Hamilton, James D. (1994a). *Time Series Analysis*, Princeton University Press.
- [13] Hayashi, Fumio. (2000). *Econometrics*, Princeton, NJ: Princeton University Press.
- [14] Johnston, Jack and John Enrico DiNardo (1997). *Econometric Methods*, 4th Edition, New York: McGrawHill.
- [15] M. A. Almeida, R. Schaeffer and E. L. La Rovere, "The Potential for Electricity Conservation and Peak Load Reduction in the Residential Sector of Brazil," *Energy*, Vol. 26, pp. 413-429, 2001.
- [16] M. A. Momani, "Factors Affecting Electricity Demand in Jordan," *Energy and Power Engineering*, Vol. 5, No. 1, pp. 50-58, 2013.
- [17] S. B. Sadineni, and R. F. Boehm, "Measurements and Simulations for Peak Electrical Load Reduction in Cooling Dominated Climate," *Energy*, Vol. 37, pp. 689-697, 2012.
- [18] S. Dudhani, A. K. Sinha, and S. S. Inamdar, "Renewable Energy Sources for Peak Load Demand Management in India," *Electrical Power and Energy Systems*, Vol. 28, pp. 396-400, 2006.
- [19] Wadjamsse Beaudelaire Djezou, PhD, "Analyse des déterminants de l'efficacité énergétique dans l'espace UEMOA" *European Scientific Journal* April 2013 edition vol.9, No.12 ISSN: 1857 – 7881 (Print) e - ISSN 1857- 7431.
- [20] Y. S. Akil, and H. Miyauchi, "Seasonal Regression Models for Electricity Consumption Characteristics Analysis," *Engineering*, Vol. 5, No. 1B, pp. 108-114, 2013.
- [21] Yusri Syam Akil, Hajime Miyauchi. Seasonal Peak Electricity Demand Characteristics: Japan Case Study. *International Journal of Energy and Power Engineering*. Vol. 2, No. 3, 2013, pp. 136-142. doi: 10.11648/j.ijepe.20130203.18.
- [22] SIE-Cameroon, 2009. Cameroon energy information system: Report 2009. Ministry of Energy and Water resources.
- [23] SIE-Cameroon, 2010. Cameroon energy information system: Report 2010. Ministry of Energy and Water resources.
- [24] R. Starts, EViews Illustrated for Version 7.2, 1st Ed., (2012) Micro Software, LLC, 2012.